HTML ABSTRACT + LINKS

Peeling mode relaxation ELM model

C. G. Gimblett

EURATOM/UKAEA Fusion Association, Culham Science Centre Abingdon, Oxon, OX14 3DB, United Kingdom

Abstract.
This paper discusses an approach to modelling Edge Localised Modes (ELMs) in which toroidal peeling modes are envisaged to initiate a constrained relaxation of the tokamak outer region plasma. Relaxation produces both a flattened edge current profile (which tends to further destabilise a peeling mode), and a plasma-vacuum *negative current sheet* which has a counteracting stabilising influence; the balance that is struck between these two effects determines the radial extent (r_E) of the ELM relaxed region. The model is sensitive to the precise position of the mode rational surfaces to the plasma surface and hence there is a 'deterministic scatter' in the results that has an accord with experimental data. The toroidal peeling stability criterion involves the edge pressure, and using this in conjunction with predictions of r_E allows us to evaluate the ELM energy losses and compare with experiment. Predictions of trends with the edge safety factor and collisionality are also made.

Keywords: Tokamak, peeling mode, relaxation, current sheet, ELM.
PACS: 52.55.Fa, 52.55.Tn

INTRODUCTION

It is now a routine observation that tokamaks undergo the so-called 'L-H' transition during which the plasma outer region develops localised steep gradients in both current density and pressure [1]. Subsequently, quasi-cyclic disturbances of the plasma edge called Edge Localised Modes (ELMs) are seen to develop [2, 3]. ELMs are repetitive disturbances in the outer region of tokamak plasmas that are influential in determining present and future tokamak performance. The explosive transient heat power flux on to external structures that is associated with ELMs raises critical issues for tokamak design, and in particular for the plasma facing components of the main vacuum chamber wall and divertor in the ITER device [4]. The ideal magnetohydrodynamic (MHD)'peeling' and 'ballooning' instabilities, driven by these edge current density and pressure gradients, have often formed the basis of theoretical explanations of ELMs [2, 5, 6]. Codes which seek to integrate these stability considerations into a systematic predictive model have also been developed [7–10].

In the following sections we first give some brief general arguments concerning the relative characteristics and importance of ballooning and peeling modes. This is followed by a discussion of the development of relaxation theory as applied to annular plasmas. We then outline a theory of the ELM instability [11] that uses a combination of peeling and relaxation ideas, and demonstrate how predictions from the model can be applied to experimental data.

CP871, *Theory of Fusion Plasmas: Joint Varenna-Lausanne International Workshop,*
edited by J. W. Connor, O. Sauter, and E. Sindoni
© 2006 American Institute of Physics 978-0-7354-0376-5/06/$23.00

Downloaded 24 Aug 2011 to 194.81.223.66. Redistribution subject to AIP license or copyright; see http://proceedings.aip.org/about/rights_permissions

PEELING-BALLOONING MODES

Ballooning modes are pressure driven instabilities localised to regions of unfavourable curvature by toroidal coupling. A simple argument that equates the pressure gradient ($-dp/dr$) energy available for toroidal magnetic curvature instability drive ($\sim -(1/R_0)dp/dr$ with R_0 the major radius) with the counteracting energy required for field line bending ($\sim k_\parallel^2 B_0^2$ with $k_\parallel$ the parallel wave number and B_0 the toroidal field) leads to an order of magnitude estimate of the pressure gradient required for ballooning as

$$\alpha \;=\; -2(\mu_0 R_0 q^2/B_0^2)\, dp/dr \;\;=\;\; \mathscr{O}(1)\,, \tag{1}$$

where q is the well-known safety factor. Ballooning stable regions are then often plotted in an '$s-\alpha$' diagram, where the shear $s=(r/q)dq/dr$ [12]. Peeling modes, on the other hand, are edge current driven, flute like in nature and cylindrical in origin. Indeed, in the cylindrical limit, a plasma with edge current density J_a that is in the same direction as the total plasma current I_p is ideal MHD peeling unstable [13](see the comment under Eq. (6)). The peeling mode can also be described as an edge localised ideal kink [13] driven by the differential torque formed by the non-zero J_a being immediately adjacent to the current-free vacuum region. This torque reinforces the initial perturbation if J_a is in the same direction as I_p. A further ingredient in a localised peeling mode is the existence of a plasma resonance (where the pitch of the perturbation equals that of the equilibrium) just outside the plasma-vacuum $\mathscr{P}/\mathscr{V}$ interface. In any actual toroidal equilibrium configuration, the prevalent instability can be an admixture of the two, as numerical investigations with codes such as ELITE have demonstrated [14]. In fact, depending on the plasma shaping, and current/pressure profile investigated the most restrictive modes are typically hybrid peeling-ballooning modes with moderate toroidal mode number ($n\sim 10$) [15].

The equilibrium pressure gradient, as well as being the direct drive behind ballooning modes, can also be seen to have a diverse role in mediating peeling-ballooning modes. This is due to the fact that in toroidal magnetic geometry some plasma particles encounter mirror fields and cannot circulate freely - the so-called trapped particles. In particular, trapped particles in the presence of a pressure gradient give rise to the well-known 'bootstrap' current

$$\mu_0 J_B \;\sim\; -2\frac{\varepsilon^{1/2}}{B_\theta}\mu_0\frac{dp}{dr} \;\;=\;\; \frac{B_0}{R_0}\frac{\alpha}{\varepsilon^{1/2}q}\,, \tag{2}$$

with ε the torus aspect ratio. This current, which is especially pronounced at the location of the steep pressure gradients to be found in the edge pedestal region of an H-mode plasma, must be taken into account in any equilibrium calculation. The subsequent effect on ballooning stability can then be seen from the following simple argument. Ampère's law can be written

$$\mu_0 J \;=\; \frac{B_0}{R_0}\frac{1}{r}\frac{d}{dr}\left(\frac{r^2}{q}\right) \;\;=\;\; \frac{B_0}{R_0}\frac{(2-s)}{q}\,, \tag{3}$$

Downloaded 24 Aug 2011 to 194.81.223.66. Redistribution subject to AIP license or copyright; see http://proceedings.aip.org/about/rights_permissions

and if we ask that this current be provided entirely by the bootstrap effect then Eqs. (2) and (3) give

$$\alpha \;=\; \varepsilon^{1/2}(2-s)\;. \tag{4}$$

Now, low shear equilibria are generally less prone to ballooning [16] and in the large aspect ratio $s-\alpha$ diagram, ballooning instability disappears completely for $s<0$ [17]. Equation (4) shows that this inequality occurs whenever

$$\alpha \;>\; 2\varepsilon^{1/2}\;, \tag{5}$$

which is a modest requirement on the pressure gradient. These simple arguments show that whilst plasma pressure is the direct drive behind ballooning instabilities, self-consistent equilibria incorporating the accompanying bootstrap current will display a reduced local shear and tend to diminish the ballooning unstable domain.

As already remarked, the peeling mode is not driven by pressure and would operate even in a pressure-less cylindrical plasma. Nevertheless, when considering the toroidal stability problem, pressure will exert an influence on the mode via toroidal coupling. In fact, the stability condition for peeling modes (in the case of a large aspect ratio circular plasma) is given by [18, 19]

$$\alpha\left\{\frac{r}{R_0}\left(1-\frac{1}{q^2}\right)+s\frac{d\Delta_{sh}}{dr}-\mathscr{F}_t\frac{sR_0}{2r}\right\} \;>\; sqR_0\frac{J_a}{B_0}\;. \tag{6}$$

Here the left hand side of the inequality expresses the effect of toroidicity on the peeling mode, and if it is absent we are left with the result referred to above concerning the relative sign of the edge and total plasma current. The quantity Δ_{sh} is the well-known equilibrium Shafranov shift, and $\mathscr{F}_t$ is a quantity related to the fraction of trapped particles. The pressure gradient terms on the left hand side of Eq. (6) represent, respectively, the stabilising effect of favourable average curvature (Mercier), a stabilising contribution from the Pfirsch-Schlüter currents ($\propto d\Delta_{sh}/dr$) and a destabilising contribution from the ($\mathscr{F}_t$ dependent) bootstrap. The first two effects would typically serve to stabilise peeling, while the third indicates that the mode will be more unstable as the plasma collisionality decreases. This stability criterion applies to a 'limiter' plasma; however most observations of H-mode occur when the plasma is surrounded by a divertor field with single or double null X-points. In this case a separatrix is induced and the question of the effect of this on peeling modes arises. This is a long-standing analytical problem, although a recent numerical study has strongly suggested that the peeling mode can be stabilised by the presence of a separatrix [20]. We will return to this point in the Discussion section.

RELAXED STATE PLASMAS AND SKIN CURRENT FORMATION

Plasma instabilities release available magnetic potential energy; as such it is natural to enquire what the final end state of such a process might be. A formulation of this problem that involved identifying a constraint characterising the behaviour of a highly

Downloaded 24 Aug 2011 to 194.81.223.66. Redistribution subject to AIP license or copyright; see http://proceedings.aip.org/about/rights_permissions

conducting plasma, namely the global magnetic helicity, was given by Taylor [21]. The minimum magnetic energy state obtained obeyed

$$\nabla \times \mathbf{B} \;=\; \mu \mathbf{B}, \;\; \mu \;\; \text{uniform}, \tag{7}$$

and had the unusual property that for $\mu a \sim \mathscr{O}(1)$ (in a perfectly conducting cylinder of radius a) the edge toroidal field became negative, thus explaining the remarkable defining characteristic of a Reversed Field Pinch (RFP)[22] plasma. The theory subsequently offered explanations for the occurrence in an RFP of helical current limiting equilibria at high μa, the interesting behaviour of the applied volts/plasma current curve in the Multipinch experiment, and led to ideas concerning non-inductive current drive (helicity injection) [23, 24].

Simply having magnetic energy available does not imply that the relaxed state is actually accessible. The RFP is 'blessed' with a range of resistive MHD modes which ensure that it is a true relaxing plasma system. For instance, the very existence of the zero in the toroidal field implies a dense set of rational surfaces on which many tearing modes can develop [25]. Also, as the poloidal field is of the same order as the toroidal field, the average curvature is everywhere unfavourable and the resistive 'g' mode can similarly be destabilised [26].

The tokamak, with a dominant toroidal field and $\mu a \sim \mathscr{O}(\varepsilon)$, has none of these modes generally available, possibly contributing to its present ability to outperform other confinement devices. Nevertheless, when the central safety factor q_0 drops below unity in a tokamak (due to current diffusion) the well-known internal kink mode stability limit is crossed [12], and furthermore the average curvature again becomes unfavourable. It has been suggested that the combination of these two instabilities could lead to a Taylor relaxation and provide an explanation of the ever-present core sawtooth fluctuations [27]. Another potential location of MHD instability is of course the tokamak plasma edge where the peeling/ballooning modes as described above are located. This is particularly true in the H-mode where steep equilibrium gradients and ELMs are encountered. These facts provide the motivation for the ELM model [11, 28] we outline in the next section.

We will be arguing that relaxation only takes place across a region where instabilities are active, and will only cease when all possible modes are stable in the new relaxed equilibrium. The formulation of such a model will obviously require an extension of the original Taylor calculation for the RFP, which assumed that the relaxation occurred everywhere. Accordingly, we may anticipate that discontinuities in the magnetic field (*i.e.* current sheets) will arise across any boundaries between relaxed and non-relaxed plasma regions [1]. This observation, in the context of highly conducting laboratory plasmas, is not new, and has been made by *e.g.* Moffatt [30] and Spies *et al.*[31]. The idea is indeed very familiar in astrophysics, where Parker [32, 33] showed that the appearance of magnetic discontinuities were inevitable in equilibrium plasmas with a given fixed topology. The idea has found particular application in solar physics, where the subsequent dissipation of current sheets formed by photospheric foot-point motion is used to explain coronal heating.

[1] This also holds true for the final state of the well-known Kadomtsev sawtooth model [29]

Downloaded 24 Aug 2011 to 194.81.223.66. Redistribution subject to AIP license or copyright; see http://proceedings.aip.org/about/rights_permissions

A PEELING RELAXATION ELM MODEL

The ELM model we now outline (see Refs [11, 28] for full details) takes the onset of a toroidal peeling mode as the initiating event of an ELM and does not concern itself with ballooning. For this reason, the model is best thought of for the moment as applying to 'type III' ELMs. This is because the type III regime observed experimentally occurs when the plasma has just entered the H mode of operation and the pressure gradient can often be seen to be below the critical value required for ballooning instability. We could also imagine the model to apply whenever Eq. (5) is satisfied and the plasma is ballooning stable.

At first sight it does not appear promising to relax an outer plasma region and then look for peeling stability. This is simply because a relaxed (flattened) current profile would have a larger edge current density J_a (at least for equilibrium current profiles that are monotonic decreasing as the edge is approached, see Fig. (1)), and this is the very factor that drives peeling instability. However, as we have discussed above, there will also be a skin current $\mathscr{K}_a$ generated by the relaxation, and this will have a separate effect on peeling mode stability. Now, increasing J_a would normally be associated with increasing $B_{\theta a}$ and hence a decreased q_a in the plasma. It follows that the jump in q across the $\mathscr{P}/\mathscr{V}$ interface is positive and $\mathscr{K}_a$ will generally be *negative*. It turns out that this has a stabilising effect on peeling, and a balance between the stabilising and destabilising effects is struck when the relaxation has extended a finite distance into the plasma. It is this fact that we will exploit to determine the model ELM widths.

Extended Taylor calculation

We must first consider the extended relaxed state calculation that is required. The relaxed state will occupy an annular region that extends from the $\mathscr{P}/\mathscr{V}$ surface at $r=a$ in to an as yet undetermined inner radius r_E. As in the Taylor formulation we will require the magnetic energy in this region to be minimised subject to its total helicity being conserved. In the tokamak ordering the equilibrium toroidal field (and its total flux) remains unchanged, and so only poloidal field energy is involved. Because an annulus has a different topology to a cylinder that includes the origin, we will have to invoke one other invariant to close the system. It is natural to invoke the total poloidal flux $\Psi_\theta = \int B_\theta dr = \int_{r_E}^{a} (r/q) dr$ as this plays an analogous role to the toroidal flux in this geometry. With due consideration to the multiply connected nature of the topology [24] it transpires that the helicity is given by

$$K \;=\; \int_V \mathbf{A}.\mathbf{B} dV \quad \propto \quad \int_{r_E}^{a} \frac{r}{q}\left(r^2 - r_E^2\right) dr \,. \tag{8}$$

Now we must minimise

$$W_\theta \;=\; \frac{1}{2\mu_0}\int_V B_\theta^2 dV \quad \propto \quad \int_{r_E}^{a} (r^3/q^2) dr \,, \tag{9}$$

Downloaded 24 Aug 2011 to 194.81.223.66. Redistribution subject to AIP license or copyright; see http://proceedings.aip.org/about/rights_permissions

subject to conservation of *both* K and Ψ_θ. This is a standard problem in the calculus of variations, so with $\lambda_{1,2}$ Lagrangian multipliers

$$W_\theta - \lambda_1 K - \lambda_2 \Psi_\theta \quad \propto \quad \int_{r_E}^{a} \left[\frac{r^3}{q^2} - \lambda_1 \frac{r}{q}\left(r^2 - r_E^2\right) - \lambda_2 \frac{r}{q} \right] dr \tag{10}$$

has to be made stationary, with solution

$$q^f(r) \quad = \quad \frac{r}{Cr + D/r} \tag{11}$$

in $r_E < r < a$ (the superscript f denotes the final relaxed profile while C, D are constants to be determined). As may have been anticipated, Eq. (11) simply gives a uniform current density as the relaxed state.

System equations

When the relaxation starts and pressure is removed from the outer plasma, then toroidal coupling is lost ($\alpha \to 0$ in Eq. (6)) and the underlying torque balance $\nabla \times (\mathbf{J} \times \mathbf{B}) = \mathbf{0}$ is essentially cylindrical and given by the well-known 'tearing' equation for the poloidal flux $\psi (= r b_r)$

$$\frac{d}{dr}\left(r \frac{d\psi}{dr} \right) - \frac{m^2 \psi}{r} \quad = \quad \frac{m}{F} \mu_0 \frac{dJ}{dr} \psi \, , \tag{12}$$

where

$$F \quad = \quad \frac{B_\theta}{r}\left(m - nq\right) \; = \; m \frac{B_0}{R_0}\left(\frac{1}{q} - \frac{n}{m} \right) \, . \tag{13}$$

The standard perturbation spatial dependence $\sim \exp i(m\theta + n\phi)$ is assumed, where m and n are the mode poloidal and toroidal wave numbers respectively.

Now as discussed above, we must allow for the existence of skin currents located at both $r = a$ and $r = r_E$. These occur simply because we are taking the fields outside the annulus to be unaffected by the relaxation and so inevitably there will exist discontinuities in the equilibrium B_θ (and hence q) at these locations. Figure (1) gives a schematic of the post-ELM model configuration. The boundary conditions on Eq. (12) follow from requiring (a) that the tangential stress is continuous and (b) that the total magnetic field have no normal component in the perturbed boundaries, *i.e.* that the perturbed material surfaces remain flux surfaces. Condition (a) can in principle be formulated by integrating Eq. (12) across the interfaces. However, care must be taken as the right hand side involves both a step in F and a step and skin current in J! In fact, we may first multiply Eq. (12) by F [28] and then integrate to find that at $r = r_E$ and a

$$\left[\left[F^2 \frac{d}{dr}\left(\frac{\psi}{rF} \right) \right] \right]_-^+ \quad = \quad 0 \, , \tag{14}$$

Downloaded 24 Aug 2011 to 194.81.223.66. Redistribution subject to AIP license or copyright; see http://proceedings.aip.org/about/rights_permissions

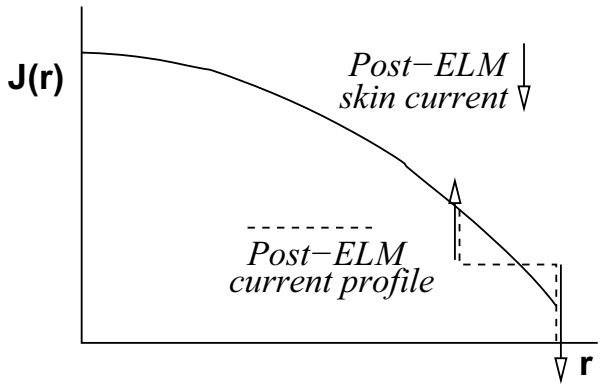

FIGURE 1. A schematic of the post-ELM current profile.

where $[[\ldots]]$ denotes a radial 'jump'. Condition (b) requires that the quantity ψ/F is continuous across $r = r_E$ and $r = a$.

All the components for deriving a controlling set of equations are now in place and as the algebra proceeds, various quantities representing the physical quantities involved arise. These are

$$\Delta_j \;=\; \left(\frac{1}{q_j} - \frac{n}{m}\right) , \tag{15}$$

a dimensionless expression of the 'distance' between a radial position j and the resonance where $n = mq$ (for peeling modes a resonance characteristically occurs just outside the $\mathscr{P}/\mathscr{V}$ interface and so Δ_a would be a small positive real number [34]),

$$\begin{aligned} I &= R_0\mu_0 J/B_0 \\ &= \frac{1}{r}\frac{d}{dr}\left(\frac{r^2}{q}\right) \end{aligned} \tag{16}$$

relating the toroidal current density to the safety factor q,

$$\mathscr{K}_j \;=\; \frac{R_0}{aB_0}\mu_0\mathscr{I}_{js} \;=\; \left[\left[\frac{1}{q}\right]\right]_{j-}^{j+} , \tag{17}$$

where $\mathscr{I}_{js}$ is the surface skin current density (the surface current per unit poloidal length, see *e.g.* Ref [35]), and

$$\Delta_j^{'} \;=\; \left[\left[\left(\frac{r}{\psi}\frac{d\psi}{dr}\right)\right]\right]_{j-}^{j+} , \tag{18}$$

the well-known jump in the perturbed poloidal flux radial derivative which is central to MHD stability analysis [25]. (The notation $\Delta^{'}$ is standard and it should be stressed that $\Delta^{'}$ is not related to the Δ defined in Eq. (15)). The system finally reduces to the following

Downloaded 24 Aug 2011 to 194.81.223.66. Redistribution subject to AIP license or copyright; see http://proceedings.aip.org/about/rights_permissions

two coupled equations that will be used to determine the unknown radius r_E (once an initial q-profile is specified, this is the only unknown quantity).

$$\Delta_a \left[\Delta_a \Delta_a^{'} + I_a\right] + \mathscr{K}_a \left[(\mathscr{K}_a - 2\Delta_a)\left(\Delta_a^{'} + m - 1\right) + 2\frac{n}{m} - I_a\right] = 0 \ , \tag{19}$$

$$\begin{aligned} &\Delta_{E-}\left[\Delta_{E-}\Delta_E^{'} + I_{E-} - I_{E+}\right] + \\ &+ \mathscr{K}_E \left[(\mathscr{K}_E + 2\Delta_{E-})\left(\Delta_E^{'} + m + 1\right) + 2\frac{n}{m} - I_{E+}\right] = 0 \ . \end{aligned} \tag{20}$$

The subscripts a and E in Eqs. (19) and (20) refer to the radial positions $r = a$ and $r = r_E$. These two radii are coupled by the relationship between $\Delta_a^{'}$ and $\Delta_E^{'}$

$$\Delta_E^{'} \ = \ -2m\frac{\left(\Delta_a^{'} + 2m\right)}{\left(g\Delta_a^{'} + 2m\right)} \ . \tag{21}$$

where $g = 1 - (r_E/a)^{2m}$. In deriving these equations we have taken solutions $\psi \sim r^{\pm m}$; this is a good approximation for $m >> 1$ (which is generally true for ELMs), and is exact in the relaxed and vacuum regions. If we choose a mode with $\Delta_a = 0$ for an initial smooth equilibrium, then Eq. (19) gives the same marginal stability condition as the pressure-free Eq. (6), namely $J_a = 0$.

It is useful to point out that the left hand side of Eq. (19) is directly proportional to $-\delta W$ [36, 37], the well-known ideal MHD energy functional.

Results for a simple initial q-profile

To provide some illustrative results we take a simple initial monotonic q-profile

$$\begin{aligned} q^i \ &= \ q_0 + (q_a - q_0)\, r^2, \ 0 \le r \le 1 \ , \\ &= \ q_a r^2, \ r \ge 1 \ . \end{aligned} \tag{22}$$

Equation (19) shows instability of the initial profile (for large m) if $I_a > 2m\Delta_a$, and this condition yields (for a fixed (q_0, q_a)) a sequence of unstable (m,n) pairs. For each member of this sequence we can solve Eqs. (19), (20) and (21) anticipating a real positive solution for the unknown ELM width $d_E = (a - r_E)/a$. (In fact examination of Eq. (19) shows that, at least for small d_E, the term involving the edge current will give a destabilising term $\sim d_E$ while the skin current, $\mathscr{K}_a$, term gives a stabilising term $\sim d_E^2$). Figure (2) shows an example of one such calculation $(q_0, q_a) = (1, 4.587)$), while Fig. (3) gives the corresponding d_E plotted against n for all the initially unstable (m,n) pairs that this choice of (q_0, q_a) provides. For this particular case Fig. (3) shows that the maximal d_E corresponds to the smallest n value, though this is not necessarily true in general. We may next compute the maximal d_E values (and their associated (m,n)) as we vary q_a, holding q_0 fixed at unity. The result is shown in Fig. (4). Corresponding to

Downloaded 24 Aug 2011 to 194.81.223.66. Redistribution subject to AIP license or copyright; see http://proceedings.aip.org/about/rights_permissions

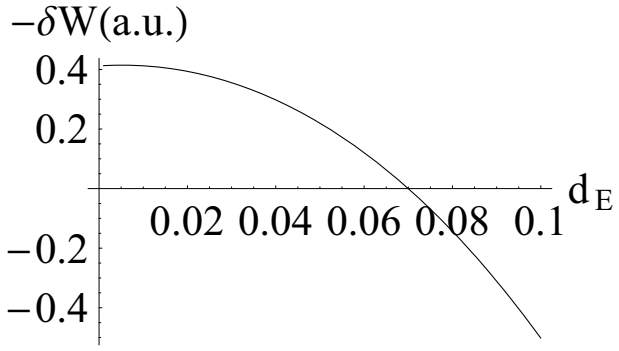

FIGURE 2. An example of locating a marginal radial position d_E for the ELM model. Here $(q_0, q_a, m, n) = (1.0, 4.587, 23, 5)$ and there is a zero of δW at $d_E = 0.0702$.

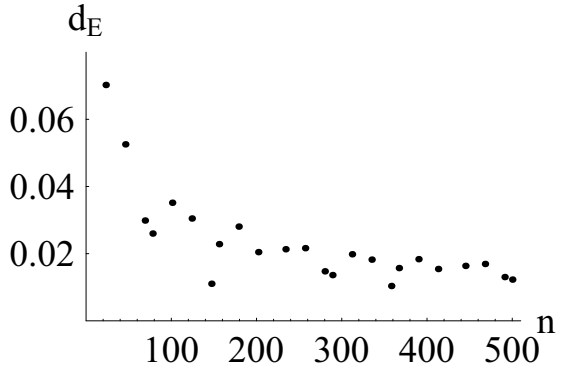

FIGURE 3. Marginally stable model ELM widths plotted against unstable n numbers for a fixed $(q_0, q_a) = (1.0, 4.587)$. The largest d_E corresponds to the zero of δW in Fig. (2).

each of the maximal d_E values of Fig. (4) is an n value, and this is plotted against q_a in Fig. (5).

An immediate impression gained from Figs. (3) to (5) is the seeming 'scatter' in the results, which is perhaps surprising as the initial profile chosen is a smooth well-behaved function. The scatter can be traced to the evaluation of the Δ quantities of Eq. (15). The discrete nature of the m/n when m and n are restricted by periodicity requirements to be integer means that the Δ quantities exhibit highly detailed structure. The 'scatter' apparent in Fig. (4) is in fact due to the discreteness of the plot, as is demonstrated in Fig. (7) where we show a high resolution version of Fig. (4) for a smaller q_a range. We see that the actual curve is comprised of multiple overlapping regions. It is tempting to ascribe the reported experimental scatter in many ELM measurements to just this effect - the actual ELM size depends critically on the 'distance' of the plasma edge q_a to a rational approximation. Figure (6) gives an experimental plot of the measured saturated ion current from a MAST edge probe, acquired during ELM activity, which demonstrates the scattered nature of much ELM data. We can find a smooth envelope that approximates to the maximal d_E of Fig. (4) by expanding the

Downloaded 24 Aug 2011 to 194.81.223.66. Redistribution subject to AIP license or copyright; see http://proceedings.aip.org/about/rights_permissions

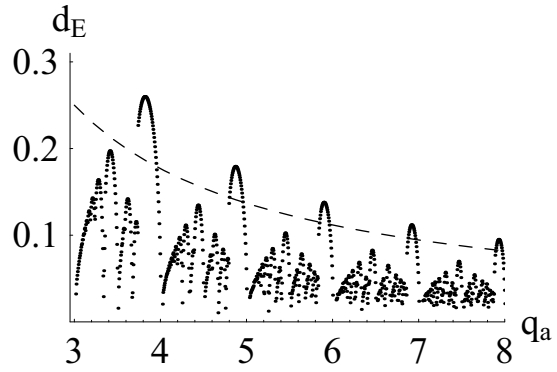

FIGURE 4. The maximal marginal d_E, plotted against initial edge q_a value. The dashed curve gives an analytic approximation for $d_E(\max)$ in the case $n = 1$ (see Eq. (23)).

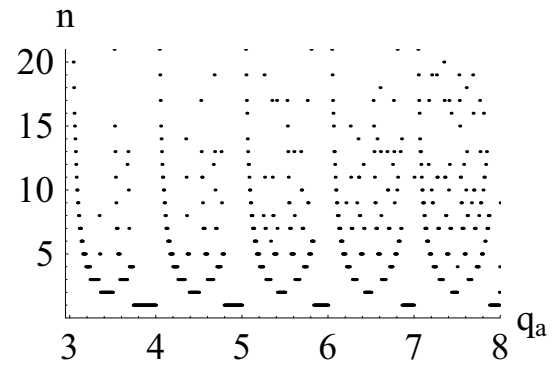

FIGURE 5. The toroidal mode numbers n that give the maximal marginal d_E values of Fig. (4), plotted against the initial edge q_a value.

entire set of determining equations (Eqs. (19) to (21)) and assuming small d_E. Two cases present themselves depending on the ordering of I_a. We take $I_a \sim \mathcal{O}(1)$ and perform the maximisation of d_E analytically to find

$$d_E^2(max) \;=\; -\frac{3}{4n}\frac{I_a^2}{(aI_a')} \tag{23}$$

($' \equiv d/dr$), and this curve is shown for $n = 1$ as the dashed line in Fig. (4). The actual width of an ELM disturbance is perhaps not a well defined experimentally measurable quantity. However, the energy losses associated with an ELM are better documented. Armed with our predictions of ELM widths we may use the assumed trigger, namely a toroidal peeling mode with stability criterion given by Eq. (6), and proceed to calculate the model ELM energy losses. Equation (6) yields a critical pressure gradient p_a' and let us take the pressure profile to be flat in the plasma core ($= p_0$), descending to zero over a distance $\delta = -p_0/p_a'$. Taking d_E from Fig. (4) and assuming pressure is lost in this outer width, we may calculate $\Delta W_{ELM}/W_{PED}(\sim d_E^2/\delta)$, where ΔW_{ELM} is the (pressure) energy lost in an ELM and W_{PED} is the total plasma energy assuming that the equilibrium

Downloaded 24 Aug 2011 to 194.81.223.66. Redistribution subject to AIP license or copyright; see http://proceedings.aip.org/about/rights_permissions

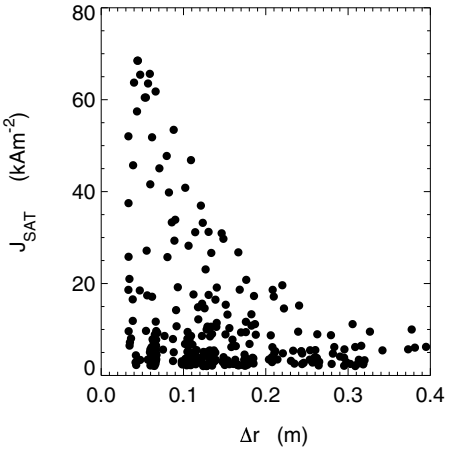

FIGURE 6. The saturated ion current from a MAST edge probe.

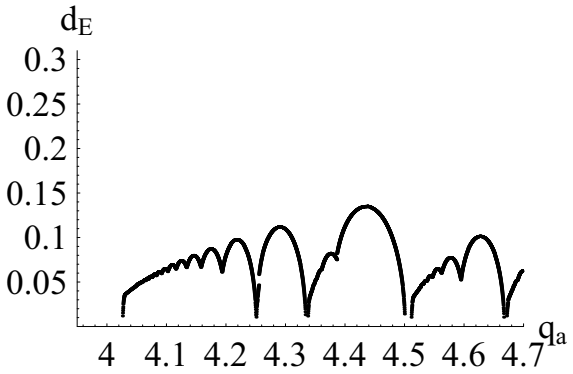

FIGURE 7. High resolution detail of the maximal d_E against q_a of Fig. (4).

pressure is p_0 everywhere [38]. Figure (8) shows the result of such a calculation where we have taken typical MAST values [38] and assumed a collisional edge plasma ($\mathscr{F}_t = 0$ in Eq. (6)). Characteristic values of a few percent are indicated, and this agrees well with the reported MAST experimental data [38].

As the plasma becomes less collisional the presence of the $\mathscr{F}_t$ term in Eq. (6) implies that the marginally stable edge pressure gradient (α) increases. Therefore, we may expect that ELM energy losses from a less collisional plasma would be higher. This trend has been reported (at least for type I ELMs) in the JET experiment [39].

DISCUSSION

We have presented a model for (type III) ELMs based on ideas derived from peeling mode and relaxation theory. With no fitted parameters, it is shown that the balance that is struck between a destabilising increase in edge current and the stabilising formation of an edge current sheet produces ELM widths (and hence plasma ELM losses) that

Downloaded 24 Aug 2011 to 194.81.223.66. Redistribution subject to AIP license or copyright; see http://proceedings.aip.org/about/rights_permissions

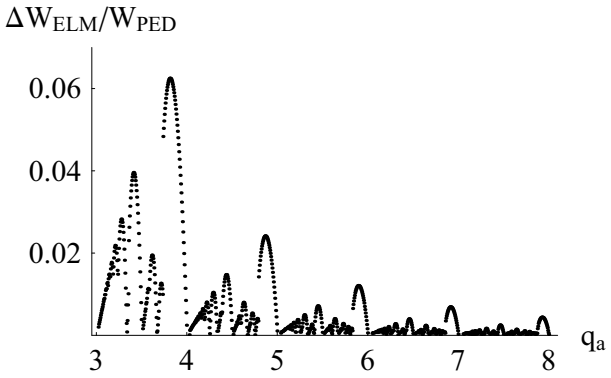

FIGURE 8. Normalized ELM energy loss $\Delta W_{ELM}/W_{PED}$ of the initial parabolic q profile (Eq. (22)) against edge safety factor q_a ($q_0 = 1$). Parameters of a characteristic MAST plasma [38] have been taken, with an aspect ratio of 1.5 and a highly collisional edge ($\mathscr{F}_t = 0$ in Eq. (6)).

are in good general agreement with experimental observations. Results from the model exhibit a sensitivity to the precise position of the edge plasma with respect to low order rational approximations, leading to a seeming 'scatter'. Arguing from the toroidal peeling stability criterion, losses become larger with decreasing collisionality.

An objection to this model is the recent result [20] that $n = 1$ ideal MHD peeling modes appear to be stabilised by the presence of a separatrix, and are replaced by a 'peeling-tearing' counterpart. An argument that could be used to support this result is that as a separatrix is approached, the safety factor q will tend to infinity and so a resonant surface is then present in an ideal plasma, producing the stabilisation. In fact, the infinity in q is approached logarithmically and so the new resonance is very close to the separatrix, perhaps making the argument vulnerable to the presence of small error fields. Also, the modes discussed in Ref. [20] are mainly limited to having zero edge current, and the drive for them comes from edge current gradients. These modes are not considered in this paper.

Our model has only been applied to a simple monotonic q-profile. It is well known that in H-mode, the neo-classical bootstrap current driven by the steep edge pressure gradient will strongly affect the shape of the equilibrium current density profile [40], and the effect of this on the model predictions needs to be investigated. However, it has been shown that self-consistent incorporation of the bootstrap current into the equilibrium reduces magnetic shear and hence the ballooning mode instability domain.

The surface negative current sheet produced by the relaxation process in this model will itself be inevitably resistively unstable. We may speculate that the explosive filament structures observed on MAST [41] to accompany an ELM are a concomitant of the break up of this current sheet.

ACKNOWLEDGMENTS

I thank many people within UKAEA Fusion, Culham for advice and discussion on ELM issues. In particular, Jim Hastie and Per Helander have been invaluable colleagues. This

Downloaded 24 Aug 2011 to 194.81.223.66. Redistribution subject to AIP license or copyright; see http://proceedings.aip.org/about/rights_permissions

work was funded jointly by the United Kingdom Engineering and Physical Sciences Research Council and by the European Communities under the contract of Association between EURATOM and UKAEA. The views and opinions expressed herein do not necessarily reflect those of the European Commission.

REFERENCES

1. H. Zohm, Plasma Phys. Control. Fusion **38**, 105 (1996).
2. J. W. Connor, Plasma Phys. Control. Fusion **40**, 191 (1998).
3. G. T. A. Huysmans, Plasma Phys. Control. Fusion **47**, B165 (2005).
4. R. Aymar *et al.*, Nucl. Fusion **41**, 1301 (2001).
5. P. B. Snyder *et al.*, Phys. Plasmas **9**, 2037 (2002).
6. T. Onjun *et al.*, Phys. Plasmas **12**, 012506 (2005).
7. Yu. Igitkhanov *et al.*, Plasma Phys. Control. Fusion **40**, 837 (1998).
8. J. S. Lönnroth *et al.*, *Proc. 29th European Physical Society Conference on Plasma Physics and Controlled Fusion (Montreux, 2002)*.
9. A. Y. Pankin *et al.*, Plasma Phys. Control. Fusion **47**, 483 (2005).
10. A. Y. Pankin *et al.*, Nucl. Fusion **46**, 403 (2006).
11. C. G. Gimblett, R. J. Hastie and P. Helander, Phys. Rev. Lett. **96**, 035006 (2006).
12. J. A. Wesson, *Tokamaks*, Oxford, Clarendon Press (1997).
13. J. A. Wesson, Nucl. Fusion **18**, 87 (1978).
14. H. R. Wilson, P. B. Snyder, G. T. A. Huysmans, and R. L. Miller, Phys. Plasmas **9**, 1277 (2002).
15. P. B. Snyder *et al.*, Phys. Plasmas **9**, 2037 (2002).
16. J. W. Connor and R. J. Hastie, Phys. Plasmas **11**, 1520 (2004).
17. O. P. Pogutse and E. I. Yurchenko, in *Reviews of Plasma Physics* Vol II (Ed. M. A. Leontovich) (Consultants Bureau, New York, 1986).
18. D. Lortz, Nucl. Fusion **15**, 49 (1975).
19. J. W. Connor, R. J. Hastie, H. R. Wilson and R. L. Miller, Phys. Plasmas **5**, 2687 (1998).
20. G. T. A. Huysmans, Plasma Phys. Control. Fusion **47**, 2107 (2005).
21. J. B. Taylor, Phys. Rev. Lett. **33**, 1139 (1974).
22. B. Alper, Phys. Fluids B, **2**, 1338 (1990).
23. J. B. Taylor, Rev. Modern Phys. **58**, 741 (1986).
24. M. K. Bevir, C. G. Gimblett and G. Miller, Phys. Fluids **28**, 1826 (1985).
25. H. P. Furth, J. Killeen and M. N. Rosenbluth, Phys. Fluids **6**, 459 (1963).
26. A. H. Glasser, J. M. Greene and J. L. Johnson, Phys. Fluids **18**, 875 (1975); *ibid* **19**, 567 (1976).
27. C. G. Gimblett and R. J. Hastie, Plasma Phys. Control. Fusion **36**, 1439 (1994).
28. C. G. Gimblett, R. J. Hastie and P. Helander, to appear in Plasma Phys. Control. Fusion, (2006).
29. B. B. Kadomtsev, Soviet Journal of Plasma Physics **1**, 389 (1976).
30. H. K. Moffatt, J. Fluid Mech. **159**, 359 (1985).
31. G. O. Spies, D. Lortz and R. Kaiser, Phys. Plasmas **8**, 3652 (2001).
32. E. N. Parker, Ap. J. **174**, 499 (1972).
33. E. N. Parker, *Cosmical Magnetic Fields. Their Origin and their Activity* (Clarendon Press, Oxford, 1979).
34. H. R. Wilson *et al.*, Phys. Plasmas **6**, 1925 (1999).
35. J. A. Shercliff, *A Textbook of Magnetohydrodynamics* (Pergamon, Oxford, 1965).
36. J. P. Freidberg, *Ideal Magnetohydrodynamics* (Plenum Press, New York and London, 1987).
37. I. B. Bernstein, E. A. Frieman, M. D. Kruskal and R. M. Kulsrud, Proc. Roy. Soc. **A244**, 17 (1958).
38. A. Kirk *et al.*, Plasma Phys. Control. Fusion **46**, A187 (2004).
39. A. Loarte *et al.*, Phys. Plasmas **11**, 2668 (2004).
40. D. M. Thomas *et al.*, Phys. Rev. Lett. **93**, 065003 (2004).
41. A. Kirk, *Proc. 33rd European Physical Society Conference on Plasma Physics and Controlled Fusion (Rome, 2006)*.

Downloaded 24 Aug 2011 to 194.81.223.66. Redistribution subject to AIP license or copyright; see http://proceedings.aip.org/about/rights_permissions